Discover Nano

RESEARCH Open Access

Camellia sinensis mediated silver nanoparticles: eco-friendly antimicrobial agent to control multidrug resistant Gram-positive *Staphylococcus aureus*

Tasneem Juzer[1†], Ranjani Soundharajan[1†] and Hemalatha Srinivasan[1*]

[†]Tasneem Juzer and Ranjani Soundharajan equally contributed to this work.

*Correspondence:
Hemalatha Srinivasan
hemalatha.sls@bsauniv.ac.in
[1]School of Life Sciences, B.S. Abdur Rahman Crescent Institute of Science and Technology, Vandalur, Chennai 600048, Tamil Nadu, India

Abstract

*Staphylococcus aureu*s provokes several clinical infections, and its treatment remains challenging due to the rise of multidrug-resistant strains. In the current scenario it's a vital need for alternative strategies to control the spread of MDR *S. aureus*. Therefore, considerable effort has been put forth to develop green nanoparticles. *Camellia sinensis* is enriched with phytocompounds with potent antibacterial properties. Green synthesis strategy is more sustainable and non-toxic compared to traditional chemical processes. CsAgNps was synthesized by mixing 1 part of fresh extract of *C. sinensis* extract with 2 parts of 1mM silver and employing photocatalytic reduction for the period of 8 h until visible colour change was observed. Synthesized CsAgNps were characterized by employing various techniques to study the size, charge, topography and elemental composition. According to the findings of the in-silico analysis, phytocompounds of *C. sinensis* including Protopine, Ellagic acid, Catechin and Techtochrysin were recognized as potential lead compounds against various virulent targets in *S. aureus*. CsAgNps were tested for its antimicrobial and antibiofilm activity in MDR and MTCC (1430). The study results showed that it controls growth and biofilm formation of strains at the concentration of 12.5 µg/mL. The potential lead compounds against various virulent targets in *S. aureus* were analyzed using in-silico technique. Future research in the development of healthcare products will focus on optimization of ecofriendly material with targeted and sustainable release and enhancing antimicrobial efficacy particularly on MDR pathogens. CsAgNps can be incorporated to develop nano-based health care products to control antibiotic resistant *S. aureus* infections.

Keywords *Camellia sinensis*, Phytoconstituents, Nanoparticles, Antibacterial efficacy, Molecular docking, *S. aureus*

1 Introduction

Nanotechnology has transformed many areas of science, delivering innovative and practical solutions to some of our toughest challenges. The advent of nanomaterials has paved the way for groundbreaking applications. As society becomes attuned to environmental concerns, the demand for environmentally friendly approaches for nanoparticle synthesis has surged. Among these approaches, biological methods stand out as some of the most eco-friendly methods of utilizing plant extracts, bacteria, and fungi to fabricate nanoparticles [1]. Metal nanoparticles exhibit unique optoelectrical properties due to their localized surface plasmon resonance, making them a subject of intense scientific investigation [2]. Among these, silver nanoparticles (AgNPs) have garnered significant attention due to their diverse applications, especially in biomedicine. The synthesis of AgNPs can be achieved through various strategies, one of which is the bottom-up approach. An eco-friendly and efficient variant of this approach is the green synthesis method of nanoparticles [3]. The research interest is growing towards synthesis of green nanoparticles for various applications in various sectors including healthcare, textiles, food and many more. Several methods including physical and chemical methods are existing however the usage of hazardous chemicals, and release of toxic byproducts limits these traditional strategies. Plant-mediated synthesis offers advantages over microbial methods, primarily attributed to the presence of phytocompounds in plant extracts that contribute to the reduction and stabilization of nanoparticles by reducing Ag + ions to Ag nanocrystals [4]. Since plant extract nanoparticles are more preferable to microorganism-based nanoparticles because they do not need specific, intricate procedures including isolation, culture management, and multiple purification stages. Additionally, there are other benefits of using plants extracts to synthesise nanoparticles, including the usage of aqueous extract, milder reaction conditions, greater practicality, and their numerous applications in healthcare applications. The green synthesis approach can use any part of the plants including leaves, flowers, stem, root, fruit, resins, gums, tubers, rhizomes etc. Plant extracts are known to contain numerous beneficial phytocompounds including flavonoids, phenols, steroids, alkaloids, terpenoids, proteins, amino acids, polysaccharides with potent antibacterial activity even in multidrug resistant organisms [5]. There are previous reports showing that the silver nanoparticles synthesized by using extracts of *Gardenia thailandica* peel, *Mangifera indica*, *Aegle marmelos*, *Citrus maxima* peel, red seaweed *Spyridia filamentosa*, vegetable waste, and *Cocos nucifera* exhibited significant antibacterial activity against *Staphylococcus aureus*, *Escherichia coli*, *Klebsiella pneumoniae*, *Acinetobacter baumannii* [6].

The emergence and rapid evolution of antibiotic-resistant bacterial pathogens, particularly Gram positive *S. aureus*, pose significant challenges to public health. These bacteria have a very adaptable nature and because of this property, they have become resistant to many antibiotics. *Methicillin-resistant Staphylococcus aureus* is one such example which makes the patient most vulnerable to several associated infections, especially hospital stays [7]. *S. aureus* is a versatile human bacterial pathogen that can cause mild to heavy infections and can sometimes be asymptomatic too. *S. aureus* bacteremia (SAB), an infection of the bloodstream, is the entry of bacteria into the bloodstream. Age plays a major role as the incidence of SAB is very high during early childhood and late adulthood. Nanoparticles can be explored as alternative treatments to treat antibiotic-resistant *S. aureus* infections. The rise of methicillin-resistant *S. aureus* exemplifies the

dire consequences of antibiotic resistance, necessitating innovative alternatives for treatment [8].

The utilization of medicinal plants for the biomedical applications particularly treating clinical isolates that exhibit multi-drug resistance is the need of the hour. The main advantages of plant based medical/ healthcare products are they are less harmful than synthetic drugs, have significant therapeutic effects, and are more cost effective. There is scientific evidence to support the idea that a number of plants contain phytocompounds that are physiologically active, and many drugs which are used in modern medicine are mimics (structural/functional similarities) of the phytocompounds that are derived from plants. Some plant extracts were believed to have strong inhibitory effects on pathogenic mDR bacteria, which could aid in the development of potent antimicrobial agents. One such plant is *Camellia sinensis*, commonly known as green tea, which is regularly consumed around the world for its numerous health benefits, including anti-inflammatory properties, immune system support, protection against heart disease and certain cancers, as well as its calming and soothing effects. The enormous health benefits of tea leaves are primarily because of their phytochemical makeup which makes it a prime option for synthesizing environmentally friendly green nanoparticles. The presence of many phytochemicals, including catechins, epigallocatechin gallate (EGCG) and other polyphenols, in *Camellia sinensis* exhibits its antibacterial, antioxidant and reducing properties [9]. These properties are especially helpful in the biosynthesis of silver nanoparticles (AgNPs), which requires reducing and stabilising agents to protect the nanoparticles from aggregation. They also help reduce silver ions (Ag+) into their metallic state. Green tea extracts have reported to have notable antimicrobial properties in Gram negative and Gram-positive bacteria [10]. The catechins and other phytocompounds which are present in *C. sinensis* have been shown to disrupt bacterial cell walls, interfere with enzyme function, and modulate the immune system, further enhancing the antimicrobial activity of the synthesized silver nanoparticles. The upsurge of multidrug-resistant (MDR) bacteria, especially in *Staphylococcus aureus*, has developed a dire need for alternative antimicrobial agents [11]. Recent studies have shown that green silver nanoparticles exhibit remarkable effectiveness in combating MDR strains, this synergy could potentially overcome the limitations posed by traditional antibiotics. Moreover, the green synthesis of nanoparticles using *C. sinensis* offers a more sustainable approach. Unlike chemical methods that often generate toxic by-products, the plant-based synthesis of silver nanoparticles is environmentally benign, contributing to a cleaner and greener approach to nanotechnology. Though there are a number of plant sources utilized for the nanoparticles synthesis, the ease of availability and its extraordinary phytochemical profile, antibacterial effect make us to select *Camellia sinensis* as the best candidate for the synthesis of ecofriendly nanoparticles to combat drug-resistant Gram-positive organisms [12].

Considering the beneficial attributes of *C. sinensis* stands out as a highly suitable plant for the biosynthesis of silver nanoparticles, offering both scientific and practical advantages in the fight against antimicrobial resistance. This study specifically explores the use of *C. sinensis*-mediated silver nanoparticles as a potential eco-friendly antimicrobial agent to control multidrug-resistant *Staphylococcus aureus*, providing new insights into the role of plant-based nanomaterials in modern medicine. Moreover, this study encompasses both in-silico and in-vitro investigations, employing molecular docking studies to

unravel the binding affinity of *Camellia sinensis* phytocompounds with various *S. aureus* virulent proteins. Subsequent in vitro studies further validate the efficacy of *Camellia sinensis*-mediated silver nanoparticles in combatting the pathogenic *S. aureus*.

2 Materials and methods

2.1 Extraction and phytochemical analysis of *Camellia sinensis* leaves extract

The fresh extracts of *Camellia sinensis* leaves were obtained from the Western Ghats. *Camellia sinensis* leaves were identified and authenticated by Dr. D. Narasimhan, a botanist based in Chennai. A specimen of the leaves was deposited at School of Life Sciences, BSACIST, Chennai (Accession number: SLS-BSAU-21008). Collected fresh leaves were cleaned and made into fine paste. 10 gm of paste was macerated overnight in 100 mL of autoclaved water. A purified extract of *Camellia sinensis* was obtained using centrifugation followed by filtration with Whatman filter paper [13, 14]. The phytochemical screening of the *Camellia sinensis* extract was carried out to test various phytochemical compounds by using the Harborne method [15]. The fresh *Camellia sinensis* leaves extract was concentrated to fine powder by using lyophilization techniques. Filtered, fresh leaf extract was brought to frozen condition by freezing the extract at − 80 °C for 12–24 h. The frozen extract was and then freeze dried into fine powder by using a freeze drier (Alpha 2–4 Ldplus, Martin Christ, Germany) at 0.013 mbar pressure and −60 °C for 8 h. Obtained lyophilized powder of leaf extract was utilized for further analysis. Lyophilized powder was dissolved in 100% methanol. 20uL of sample was injected for LC-MS analysis (Waters Xevo G2 XS QTOF) to analyze the compounds. 0.1% Formic acid in water and acetonitrile was used as mobile phase A and B respectively. MassLynx V4.1 was used to process the obtained spectrum to study the details of phytochemical composition of the fresh green *Camellia sinensis* extract.

2.2 In silico studies

From the LC-MS analysis results, 77 compounds were obtained, out of which only 30 compounds that obeyed all five of Lipinski's rules were selected and docked against our desired proteins of interest. (Table 1). These phytoconstituents along with ampicillin were selected for interactions against different bacterial proteins of the pathogen *S. aureus* (Table 2). The 3D structures of bacterial proteins were obtained from the Protein Data Bank (PDB) and the phytocompounds were downloaded in SDF format from PubChem. With the assistance of SwissADME and Lipinski's rule of 5, phytocompounds were screened to determine their similarity to pharmaceuticals. Prior to performing docking, proteins including Penicillin-binding protein mecA (PDB ID: 1VQQ) of *S. aureus*, Metallo-beta-lactamase (PDB ID: 3R2U) of *S. aureus* subsp. aureus COL, C (30) carotenoid dehydrosqualene synthase complexed with dehydrosqualene (DHS) (PDB ID: 3R2U) of *S. aureus* subsp. *aureus*, C (30) carotenoid dehydrosqualene synthase complexed with bisphosphonate BPH-830 of *S. aureus* (PDB ID: 2ZY1) were prepared using Discover studio visualizer (DSV) by removing water molecules, hetero atoms, and adding polar hydrogens. Molecular docking was performed using the PyRx software, and the results were visualized by using the Discovery studio visualizer [16–18].

Table 1 Screening the phytocompounds of *Camellia sinensis* by using lipinski's rules of 5

S. No	Compound	PubChem	Molecular weight g/mol	Water solubility Log S (ESOL)	TPSA (Å^2)	Does it obey Lipinski's rules of 5?
1.	Econazole	3198	381.68 g/mol	− 5.67	27.05 Å^2	Yes
2.	Homocysteine	91,552	135.18 g/mol	1.67	102.12 Å^2	Yes
3.	Guanidinosuccinate	439,918	175.14 g/mol	0.62	139.00 Å^2	Yes
4.	Methionine sulfoxide	847	165.21 g/mol	1.98	99.60 Å^2	Yes
5.	2-Amino-6-methoxybenzothiazole	15,630	180.23 g/mol	− 2.96	76.38 Å^2	Yes
6.	2,5-Dimethoxy-4-chloroaniline	22,833	187.62 g/mol	− 2.38	44.48 Å^2	Yes
7.	4-Methyl-5-thiazoleethanol	1136	143.21 g/mol	− 1.54	61.36 Å^2	Yes
8.	Gyromitrin	9,548,611	100.12 g/mol	− 0.15	32.67 Å^2	Yes
9.	Tartaric acid	875	150.09 g/mol	0.61	115.06 Å^2	Yes
10.	Techtochrysin	5,281,954	268.26 g/mol	− 4.39	59.67 Å^2	Yes
11.	Indole-3-ethanol	10,685	161.20 g/mol	− 1.87	36.02 Å^2	Yes
12.	Tryptophanol	6,951,149	190.24 g/mol	− 1.73	62.04 Å^2	Yes
13.	Trigonelline	5570	137.14 g/mol	− 1.39	44.01 Å^2	Yes
14.	4-Hydroxy-3-methoxycinnamic acid	445,858	194.18 g/mol	− 2.11	66.76 Å^2	Yes
15.	2-morpholinoethanesulfonic acid	78,165	195.24 g/mol	1.35	75.22 Å^2	Yes
16.	Catechin	9064	290.27 g/mol	− 2.22	110.38 Å^2	Yes
17.	Sulthiame	5356	290.4 g/mol	− 1.83	114.30 Å^2	Yes
18.	Eugenol	3314	164.20 g/mol	− 2.46	29.46 Å^2	Yes
19.	Ellagic acid	5,281,855	302.19 g/mol	− 2.94	141.34 Å^2	Yes
20.	4,9-dimethoxy-7-(perfluorobutyl)-5 H-furo[3,2-g] chromen-5-one	1,789,495	464.23 g/mol	− 5.66	61.81 Å^2	Yes
21.	1-benzylpiperazine	75,994	176.26 g/mol	− 1.96	15.27 Å^2	Yes
22.	Milrinone	4197	211.22 g/mol	− 2.03	69.54 Å^2	Yes
23.	Tilidine	30,131	273.37 g/mol	− 3.35	29.54 Å^2	Yes
24.	Protopine	4970	353.4 g/mol	− 4.13	57.23 Å^2	Yes
25.	4-acetamidobutanoate	18,189	145.16 g/mol	− 0.03	66.40 Å^2	Yes
26.	3-Methyl-1-phenyl-1 H-pyrazol-5-amine	70,801	173.21 g/mol	− 2.70	43.84 Å^2	Yes

Table 1 (continued)

S. No	Compound	PubChem	Molecular weight g/mol	Water solubility Log S (ESOL)	TPSA (Å^2)	Does it obey Lipinski's rules of 5?
27.	2-Isopropylphenyl methylcarbamate	17,517	193.24 g/mol	− 2.55	38.33 Å^2	Yes
28.	Temozolomide	5394	194.15 g/mol	− 0.79	108.17 Å^2	Yes
29.	Scopoletin	5,280,460	192.17 g/mol	− 2.46	59.67 Å^2	Yes
30.	Dihydroxyacetone phosphate	668	170.06 g/mol	0.91	113.87 Å^2	Yes
31.	Ampicillin	6249	349.40 g/mol	− 1.15	138.03 Å^2	Yes

Table 2 Virulent proteins of *S. aureus*

S. No	PDB (Protein data bank) ID	Protein molecule	Organism	Gene	Classification
1.	1VQQ	Penicillin-binding protein mecA	*S. aureus*	mecA	Biosynthetic protein
2.	3R2U	Metallo-beta-lactamase	*S. aureus subsp. aureus COL*	SACOL0046	Hydrolase
3.	3NRI	C (30) carotenoid dehydrosqualene synthase complexed with dehydrosqualene (DHS)	*S. aureus subsp. aureus A017934/97*	crtm, SHAG_00345	Transferase
4.	2ZY1	C (30) carotenoid dehydrosqualene synthase complexed with bisphosphonate BPH-830	*S. aureus*	crtM	Transferase

2.3 Synthesis and characterization of CsAgNps

Synthesis of CsAgNps was carried out in the Erlenmeyer flask containing 1:2 ratio of fresh leaves extract with 1mM AgNO3 solution (400 mL of pure *Camellia sinensis* extract in 800 mL of silver nitrate solution). The solution was combined and exposed to sunlight for photocatalytic activity (approximately 8 h) until the visible colour change was observed. After observing prominent colour change, the nanoparticles were obtained by centrifuging the colloidal solution. The pellets obtained were purified by using ethanol and then dried in a hot air furnace until a fine powder of nanoparticles was obtained. Nanoparticles were dissolved in 10% DMSO for antibacterial assays. Fine powders of the synthesized CsAgNPs were used for various characterization techniques. These included UV-Visible spectroscopy to determine optical properties and predict the SPR (Surface Plasmon Resonance) peak, FTIR (Fourier Transform Infrared Spectroscopy) analysis to identify functional groups, and DLS (Dynamic Light Scattering) with zeta potential analysis to measure particle size and surface charge. The shape and surface topography were examined using FESEM (Field Emission Scanning Electron Microscopy), while EDX (Energy Dispersive X-ray Spectroscopy) provided information on elemental composition. Crystallinity was assessed through XRD (X-ray Diffraction), and HRTEM (High-Resolution Transmission Electron Microscopy) along with SAED

(Selected Area Electron Diffraction) was used to study detailed structural features [13, 14].

2.4 Antibacterial assays

The fresh cultures of *S. aureus* 18-D and SA MTCC (1430) were grown in Luria-Bertani (LB) broth, and all the experiments were carried out at 10^6 CFU/mL (colony forming unit) [16–18]. Pathogenic strain *S. aureus* 18-D was obtained from Tagore medical college, Chennai, after obtaining proper ethical clearance (Ref. no. BSAU: REG-OFF:2016/02SLS).

2.4.1 Agar well diffusion to determine the preliminary antibacterial activity of the CsAgNps

S. aureus – 18-D and SA MTCC (1430) bacterial cultures were swabbed onto freshly prepared LB agar after 24 h of growth. Agar well diffusion was performed by placing 50 µL of 10% DMSO (blank) in one well, 75 µL of nanoparticle in one well, 50 µL of nanoparticle in another, one well as a control (25 µL of Ampicillin (1 mg/mL)) and the final well with 50 µL of diluted AgNO3 solution. After 24 h of observation, the diameters of the zones of inhibition were measured in millimetres. The organism was incubated in an incubator at 37 °C [19].

2.4.2 Bacteriostatic, bactericidal, and anti-biofilm activity of CsAgNps

The MIC (minimum inhibitory concentration) was evaluated by following the standard protocol as mentioned in the paper [17, 23–26] After 24 h of performing MIC, MBCs (minimum bactericidal concentrations) were evaluated by the surface drop method on sterile agar plates and were incubated for 24 h at 37 °C and observed. The studies were carried out in triplicates, using control (bacterial strains without any treatment), positive control with standard antibiotics treatment (bacterial strains with ampicillin treatment) and CsAgNps treatment (bacterial strains with CsAgNps treatment). In order to carry out the assays plain LB broth was maintained as blank, bacterial strain inoculated in LB broth was considered as control, bacterial strain inoculated in LB broth treated with ampicillin (25 µg/ml) as standard antibiotics treatment and bacterial strain inoculated in LB broth treated with serially diluted CsAgNps (1 mg/ml) were considered as test samples. All the assays were maintained with plain LB broth as blank to check the external contamination [20].

After 48 h, the incubated 96-well plates were dipped in water and the contents were washed and discarded gently in the water tub. It was then kept for drying. Once dried, 100 µL of crystal violet was added to all the wells and kept for 15 min in the open air. The crystal violet was discarded gently and washed with the help of a water tub. It was kept for complete drying. 150 µL of 30% glacial acetic acid (30 mL of 100% or pure glacial acetic acid in 70 mL of distilled water) was added to all the wells and the readings were taken and noted. The MIC and Biofilm values were both obtained at 595 nm using a Perkin Elmer multi-mode reader. The data was tabulated in excel, and two graphs were created: the percentage of growth at 24 h and the percentage of biofilm development. The experiments were done in triplicate, with the control (no CsAgNps) and CsAgNps treatment [21].

2.4.3 Statistical analysis

The experiments were carried out thrice in triplicates. The graphs were plotted in MS Excel, and the mean, standard deviation, and student t-test were calculated. All the values were represented by computing the mean of triplicate measurements ($n = 3$). Bars indicate the standard deviation. The student t-test was employed to determine statistical significance, and the findings were declared significant when $P < 0.01$=**. The error bars reflect ± standard deviation. **test ($P < 0.01$) [25].

3 Results and discussion

3.1 Phytochemical analysis of fresh *Camellia sinensis* leaves extract

Phytochemical screening of the fresh *Camellia sinensis* leaves extract indicated the presence of flavonoids, phenols, saponins, steroids, terpenoids, alkaloid, glycosides. *Camellia sinensis* leaf extract containing bioactive compounds including flavonoids, phenols, saponins, steroids, terpenoids, alkaloids, and glycosides exhibit anti-oxidant, anti-bacterial, anti-inflammatory, and anti-cancer properties. LC-MS analysis of fresh *Camellia sinensis* leaves extract detected the presence of 77 phytocompounds. Positive and negative mode BPI (base peak intensity) and TIC (Total Ion Chromatogram) chromatograms of *Camellia sinensis* extract are represented in Fig. 1a, b respectively. These phytocompounds of *C. sinensis* leaves extract synergistically contribute its role in nanoparticles synthesis and exhibiting its antibacterial property.

3.2 In Silico analysis of *Camellia sinensis* phytocompounds with *S. aureus* proteins

The ligand-protein interactions, structural conformations, and binding scores of *Camellia sinensis* phytocompounds with several *S. aureus* proteins were analyzed by using molecular docking (Tables 3 and 4). The high negative ΔG values imply that the ligands have a high binding affinity towards the active site of the receptor, indicating that they have antibacterial potential. Moreover, the ligands were evaluated for their absorption, metabolism, distribution, and excretion (ADME) attributes, and their drug-likeness property was determined by screening the ligands' Lipinski rule of five. The phytocompounds with the highest binding energy were also a helping hand to the CsAgNps in exhibiting the antibacterial property. (Figures 2a and b and 3a and b) Ampicillin was

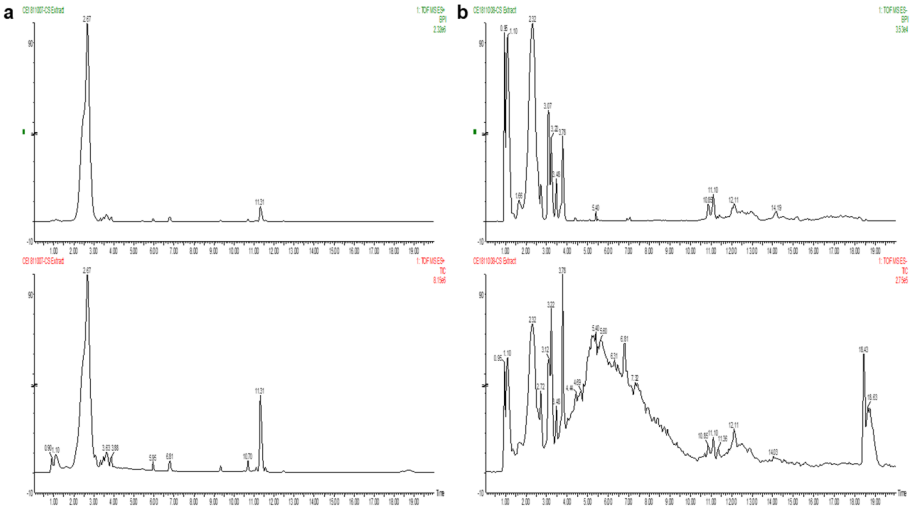

Fig. 1 BPI and TIC Chromatograms of *Camellia sinensis* extract **a** Positive mode **b** Negative mode

Table 3 Interaction of *S. aureus* proteins with phytocompounds of *Camellia sinensis*

S.No	Compound	PubChem CID	Binding energy (kcal/mol) Penicillin-binding protein mecA 1VQQ	Binding energy (kcal/mol) C (30) carotenoid dehydrosqualene synthase complexed with bisphosphonate BPH-830 2ZY1
1.	4,9-dimethoxy-7-(perfluorobutyl)-5 H-furo[3,2-g]chromen-5-one	1,789,495	− 9	− 9.8
2.	Protopine	4970	− 8.3	− 8.8
3.	Ellagic acid	5,281,855	− 8.4	− 8.6
4.	Catechin	9064	− 8.1	− 8.7
5.	Techtochrysin	5,281,954	− 7.8	− 8.8
6.	Milrinone	4197	− 7.4	− 7.7
7.	Sulthiame	5356	− 7.3	− 7.4
8.	Econazole	3198	− 7.1	− 7.7
9.	Ampicillin	6249	− 6.9	− 7.4
10.	Tryptophanol	6,951,149	− 6.4	− 7.1
11.	Scopoletin	5,280,460	− 6.6	− 7.1
12.	Temozolomide	5394	− 6.5	− 6.5
13.	2– Isopropylphenyl methylcarbamate	17,517	− 6.1	− 6.9
14.	Guanidinosuccinate	439,918	− 6.1	− 5.4
15.	4– Hydroxy– 3– methoxycinnamic acid	445,858	− 6	− 6.6
16.	Indole– 3– ethanol	10,685	− 5.8	− 6.6
17.	3-Methyl-1-phenyl-1 H-pyrazol-5-amine	70,801	− 5.8	− 6.5
18.	Eugenol	3314	− 5.6	− 6.4
19.	1-benzylpiperazine	75,994	− 5.5	− 7.1
20.	Tilidine	30,131	− 5.6	− 6
21.	Tartaric acid	875	− 5.4	− 5.6
22.	Trigonelline	5570	− 5.3	− 5.3
23.	2-Amino-6-methoxybenzothiazole	15,630	− 5.2	− 6.1
24.	2-morpholinoethanesulfonic acid	78,165	− 5.1	− 5
25.	2,5-Dimethoxy-4-chloroaniline	22,833	− 4.6	− 5.4
26.	4-acetamidobutanoate	18,189	− 4.7	− 4.8
27.	Dihydroxyacetone phosphate	668	− 4.6	− 5.3
28.	4-Methyl-5-thiazoleethanol	1136	− 4.4	− 0.4.4
29.	Methionine sulfoxide	847	− 4.4	− 4.4
30.	Homocysteine	91,552	− 4.1	− 3.9
31.	Gyromitrin	9,548,611	− 4.1	− 3.7

taken as the control and some of the phytocompounds exhibited higher binding affinity compared to the control. In *S. aureus*, various *Camellia sinensis* phytocompounds such as 4,9-dimethoxy-7-(perfluorobutyl)-5 H-furo[3,2-g]chromen-5-one, Protopine, Ellagic acid, Catechin and Techtochrysin had the lowest optimum binding energies starting from − 10 kcal/mol. (Tables 3 and 4). Thus, 4,9-dimethoxy-7-(perfluorobutyl)-5 H-furo[3,2-g]

Table 4 Interaction of *S. Aureus subsp. Aureus COL* and *S. Aureus subsp. Aureus A017934/97* proteins with phytocompounds of *Camellia sinensis*

S.No	Compound	PubChem	Binding Energy (kcal/mol) Metallo-beta-lactamase 3R2U	Binding Energy (kcal/mol) C (30) carotenoid dehydrosqualene synthase complexed with dehydrosqualene (DHS) 3NRI
1.	Protopine	4970	− 10	− 8.3
2.	4,9-dimethoxy-7-(perfluorobutyl)-5 H-furo[3,2-g]chromen-5-one	1,789,495	− 9.4	− 9.6
3.	Ellagic acid	5,281,855	− 9.5	− 8.2
4.	Techtochrysin	5,281,954	− 8.7	− 9.3
5.	Catechin	9064	− 8.6	− 8.7
6.	Sulthiame	5356	− 8.1	− 8
7.	Ampicillin	6249	− 7.9	− 8.2
8.	Econazole	3198	− 7.6	− 8.1
9.	Milrinone	4197	− 7.3	− 6.1
10.	Tilidine	30,131	− 7	− 5.6
11.	3-Methyl-1-phenyl-1 H-pyrazol-5-amine	70,801	− 6.9	− 6.3
12.	Tryptophanol	6,951,149	− 7	− 6.9
13.	2-Isopropylphenyl methylcarbamate	17,517	− 7	− 6.5
14.	Scopoletin	5,280,460	− 6.9	− 6.9
15.	Temozolomide	5394	− 6.8	− 5.9
16.	4-Hydroxy-3-methoxycinnamic acid	445,858	− 6.7	− 6.6
17.	Indole-3-ethanol	10,685	− 6.6	− 6.4
18.	1-benzylpiperazine	75,994	− 6.4	− 7.1
19.	Eugenol	3314	− 6.3	− 6.1
20.	Guanidinosuccinate	439,918	− 6.2	− 5.2
21.	2-Amino-6-methoxybenzothiazole	15,630	− 6.2	− 5.8
22.	Trigonelline	5570	− 5.6	− 5.2
23.	4-acetamidobutanoate	18,189	− 5.4	− 4.6
24.	2,5-Dimethoxy-4-chloroaniline	22,833	− 5.3	− 5.3
25.	Tartaric acid	875	− 5.2	− 5.1
26.	2-morpholinoethanesulfonic acid	78,165	− 5.1	− 5.5
27.	4-Methyl-5-thiazoleethanol	1136	− 4.8	− 4.3
28.	Dihydroxyacetone phosphate	668	− 4.8	− 5
29.	Methionine sulfoxide	847	− 4.7	− 4.4
30.	Gyromitrin	9,548,611	− 4.3	− 3.8
31.	Homocysteine	91,552	− 4.3	− 3.9

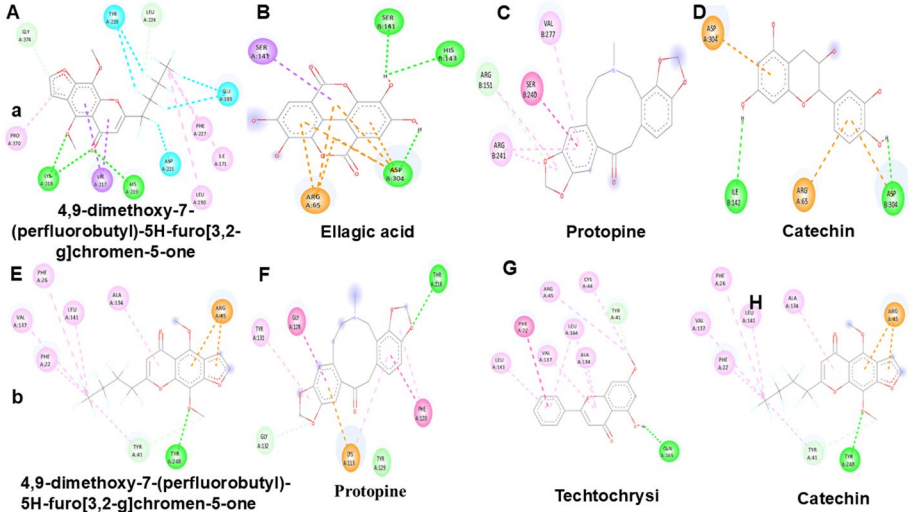

Fig. 2 2D interaction of virulent proteins of *S. aureus* with phytocompounds of *Camellia sinensis*: **a** Interactions of 1VQQ- penicillin-binding protein mecA with 4,9-dimethoxy-7-(perfluorobutyl)-5 H-furo[3,2-g]chromen-5-one **A**, Ellagic acid (**B**), Protopine (**C**), Catechin (**D**). **b** Interactions of 3R2U- Metallo-beta-lactamase with 4,9-dimethoxy-7-(perfluorobutyl)-5 H-furo[3,2-g]chromen-5-one (**E**), Protopine (**F**), Techtochrysin (**G**), Catechin (**H**)

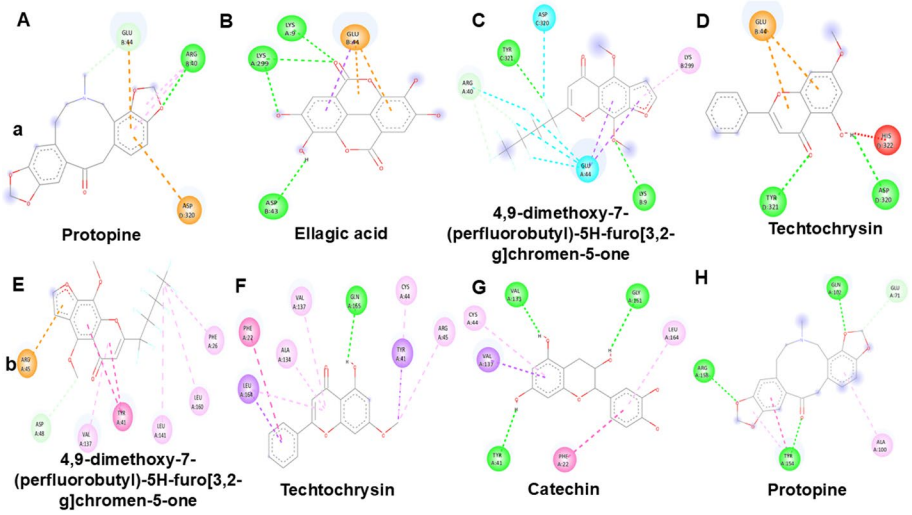

Fig. 3 2d interaction of virulent proteins of *S. aureus* with phytocompounds of *Camellia sinensis*: **a** Interactions of 2ZY1- C(30) carotenoid dehydrosqualene synthase complexed with bisphosphonate BPH-830 with Protopine (**A**), Ellagic acid (**B**), 4,9-dimethoxy-7-(perfluorobutyl)-5 H-furo[3,2-g]chromen-5-one (**C**), Techtochrysin (**D**). **b** Shows the various interactions of 3NRI- C(30) carotenoid dehydrosqualene synthase complexed with dehydrosqualene (DHS) with 4,9-dimethoxy-7-(perfluorobutyl)-5 H-furo[3,2-g]chromen-5-one (**E**), Techtochrysin (**F**), Catechin (**G**), Protopine (**H**)

chromen-5-one, Protopine, Ellagic acid, Catechin and Techtochrysin have been recognized as potential lead compounds against various proteins and enzymes in *S. aureus*.

3.3 Biogenesis and characterization of CsAgNps

Camellia sinensis leaves plant extract mediated silver nanoparticles were synthesized by employing green synthesis strategy. The phytocompounds in the fresh *Camellia sinensis* leaves extract were the prime compounds for initiating the reduction reaction during the synthesis of CsAgNps [22]. The formation of CsAgNps was initially confirmed by

the color change of silver nitrate solution from colorless to brownish wood color after the addition of purified fresh *Camellia sinensis* extract to the silver nitrate solution. UV visible spectroscopy showed the SPR peak around 400–450 nm confirming the synthesis of CsAgNps (Fig. 4a). The optical properties of the nanoparticles depend on the size of the particles. The results were consistent with the previously reported green nanoparticles synthesized by using *S. officinalis* [23]. The phytocompounds are reported to play a major role in reduction of silver nitrate during the synthesis of CsAgNps. Tea leaf extract is rich in various phytocompounds including epigallocatechin gallate (EGCG), epicatechin, epigallocatechin, epicatechin gallate, quercetin, kaempferol, ellagic acid, and gallic acid. There are reports supporting that flavonoids, phenolics play a major role in the reduction of silver nitrate and helps in the stabilization of the nanoparticles [24].

The XRD analysis of CsAgNps typically shows peaks corresponding to the (111), (200), (220), and (311) planes, aligning with the face-centered cubic (FCC) structure of silver, and these peaks are often compared with JCPDS file number 04-0783. The diffraction peaks corresponding to the (111), (200), (220), and (311) planes typically appear at 2θ values of approximately 38.2°, 44.4°, 64.6°, and 77.3°, respectively. XRD analysis confirms the crystalline nature and presence of silver in CsAgNps. The size of CsAgNps crystallite can be measured by applying Scherrer equation, where $D = K\lambda / \beta Cos\theta$ where D is the nanoparticle's crystalline size, K represents the Scherrer constant (0.98), λ denotes the wavelength (1.54), and β denotes the full width at half maximum (FWHM) [25, 26] and the crystallite size of the CsAgNps was calculated as 21.26 nm (Fig. 4b).

The zeta potential analysis of CsAgNps confirms the surface charge of -33.4 mV, conductivity of 0.0823 mS/cm (Fig. 4c). Zeta potential value implies the stability of the nanoparticles in the colloidal solution. The negative zeta value shows the electrostatic repulsion between the particles which makes the particles move apart and avoid aggregation. The literature states that stable nanoparticles have a zeta potential more than + 30 mV or less than − 30 mV. Hence the zeta potential value of CsAgNps confirms as a stable nanoparticles. The negative potential was obtained because of the capping agent that was present in the fresh leaves extract of *C. sinensis* [27].

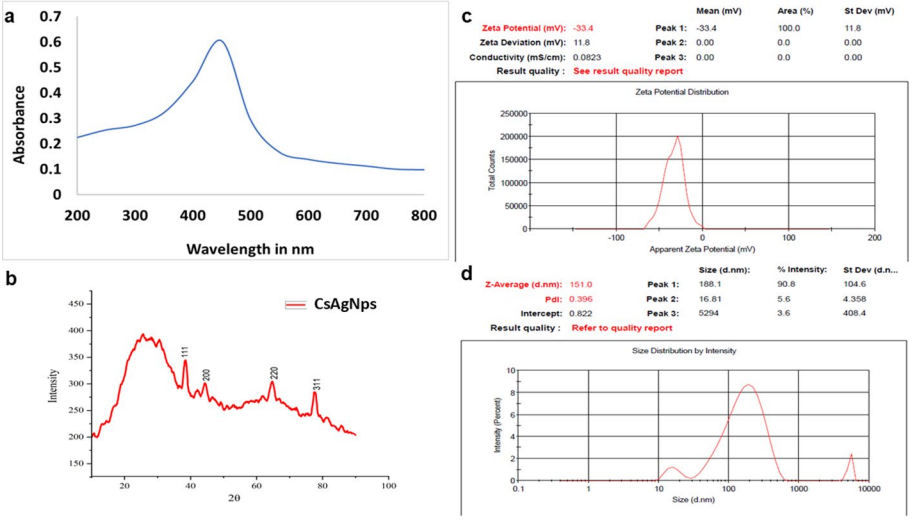

Fig. 4 Characterization of the synthesized CsAgNps: **a** UV visible spectrum of *C. sinensis* leaves extract extract mediated CsAgNps showing the SPR peak. **b** XRD spectrum of CsAgNps depicting face-centered cubic (FCC) structure, **c** Surface charge of CsAgNps obtained by zeta potential analysis, **d** Size of CsAgNps obtained by zeta sizer

The Zeta sizer was used to measure the hydrodynamic size of the nanoparticles, with the CsAgNPs showing a size of 151 d.nm (Fig. 4d). Typically, the size measured by DLS appears larger than what is observed through electron microscopy. This is because, in a colloidal solution, nanoparticles form a hydrodynamic layer around them, which leads to a larger apparent particle size when analyzing scattered light in the DLS measurement. Polydispersity index (PDI) was used to determine the homogeneity or heterogeneity of the sample based on their size. PDI value of 0 indicates monodispersity, whereas a score of 1 indicates polydispersity. According to reports, samples can be classified as monodisperse if their PDI values are less than 0.3. The PDI of value of CsAgNps was observed as 0.396 which confirms the monodisperse nature of the nanoparticles. The results were consistent with the silver nanoparticles synthesized by using *Haematococcus pluvialis* extract [28].

FTIR analysis was performed both for the extract and CsAgNps to study the functional groups which were involved in the synthesis of CsAgNps. FTIR spectrum of extract indicates the presence of peaks at 3321.78, 2921.63, 2852.2, 2164.7, 2058.64, 2015.25, 1986.32, 1616.06, 1536.02, 1449.24, 1366.32, 1230.36, 1145.51, 1032.69, 823.455, 760.78, 613.252, 420.406 cm^{-1} which corresponds to functional groups namely O-H (hydroxyl) or N-H (amine), C-H (alkane), C-H (alkane), C≡C (alkyne) or C≡N (nitrile), C≡C (alkyne), C = C = C (allene) or Overtones, Overtones or weak C = C, , C=C (alkene or aromatic), NO_2 (nitro), C-H (alkane bending), C-H (alkane bending), C-O (ether, ester), C-O (alcohol, ester), C-O (alcohol, ether), C-H (aromatic), C-H (aromatic or alkene), C-H (aromatic) or C-X (halides), C-X (halides) respectively (Fig. 5a). FTIR spectrum of CsAgNps indicates the presence of peaks at 3900.32, 3856.93, 3758.58, 3323.71, 2978.73, 2851.24, 2320.91, 2162.78, 2056.71, 1983.43, 1716.34, 1617.98, 1516.74, 1464.67, 1368.25,

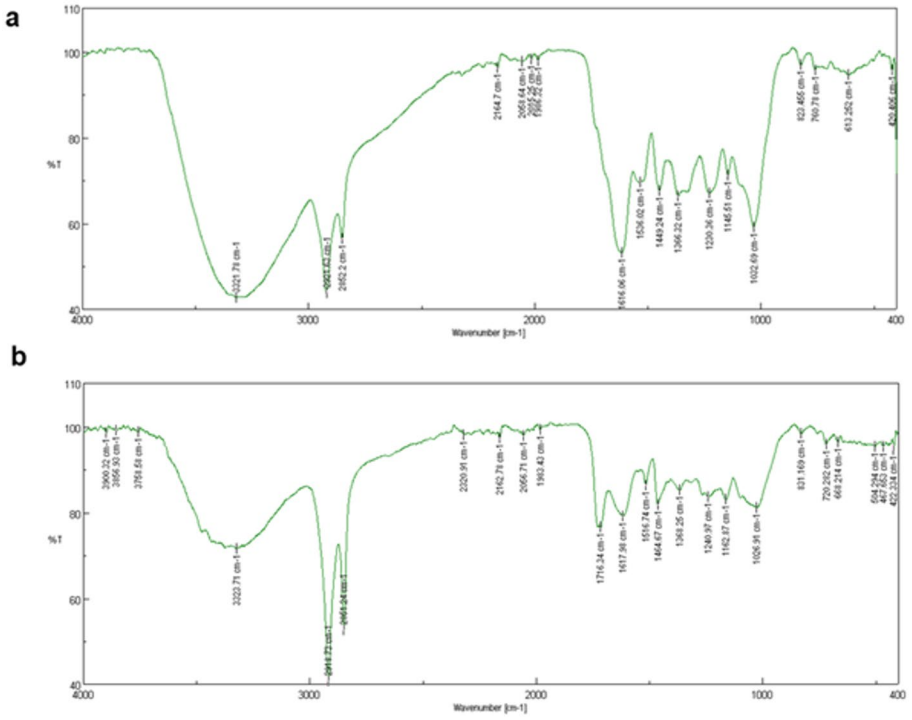

Fig. 5 Characterization of the synthesized CsAgNps by FTIR analysis: **a** FTIR spectrum of *C. sinensis* leaves extract. **b** FTIR spectrum of *C. sinensis* leaves extract mediated CsAgNps

1240.97, 1162.87, 1026.91, 831.69, 720.282, 504.294, 668.214, 467.653, 426.334 cm^{-1} which corresponds to functional groups namely O-H (strong, broad), O-H (strong, broad), O-H (sharp), N-H or O-H, C-H (alkane), C-H (alkane), C≡N or C≡C, C≡C or C≡N, C≡C (alkyne), C = C = C (Allene) or Overtones, C = O (carbonyl), C = C (aromatic or alkene), NO_2 (nitro), C-H (alkane bending), C-H (alkane bending), C-O (ether, ester), C-O (alcohol, ester), C-O (alcohol, ether), C-H (aromatic), C-H (alkane bending), C-X (halides), C-H (aromatic), C-X (halides), C-X (halides) respectively (Fig. 5b). The OH stretching represents the alcohol and phenols that were present in the leaf extract. The stretching of OH also contributed by the presence of enzymes, proteins, and carbohydrates that were present in the leaf extract. The presence of many functional groups in extract and CsAgNps indicate role of functional groups in reduction and capping during the synthesis of nanoparticles.

Similar to the leaf extract of *C. sinensis*, *C. haematocephala* also contains gallic acid. Gallic acid was reported to reduce silver ions. The OH group that is present in gallic acid forms intermediate compound and reduce the metallic silver by means of oxidation to form quinone structure. Similar to gallic acid, there are many phytocompounds responsible for reduction and capping. These phytocompounds play a predominant role in deciding the shape, size, charge, physical and biological properties, mechanism of antimicrobial action and many more [29].

FESEM image confirmed the presence of spherical shaped nanoparticles by showing the aggregates of nanoparticles which are less than 100 nm in size (Fig. 6a). The appearance of aggregation was because of sample processing steps involved during FESEM analysis. The FESEM results are consistent with the UV visible spectrum between 400 and 450 nm which corresponds to spherical shaped nanoparticles as well as the DLS also interprets the hydrodynamic size of 151 d.nm. The EDAX results of CsAgNps showed a signal peak at 3 keV and this confirmed the abundance of silver along with traces of oxygen, sulfur and carbon (Fig. 6b).

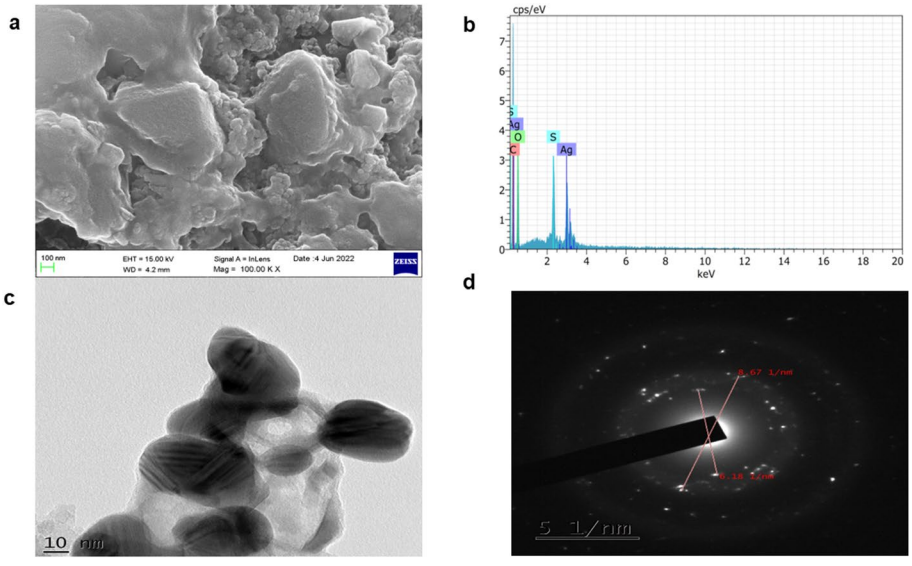

Fig. 6 Characterization of the synthesized CsAgNps: **a** Morphology of the synthesized CsAgNps by FESEM analysis. **b** EDAX results confirming the presence of silver in CsAgNps **c** Size of the synthesized CsAgNps shown through HR-TEM results. **d** SAED results of the synthesized CsAgNps

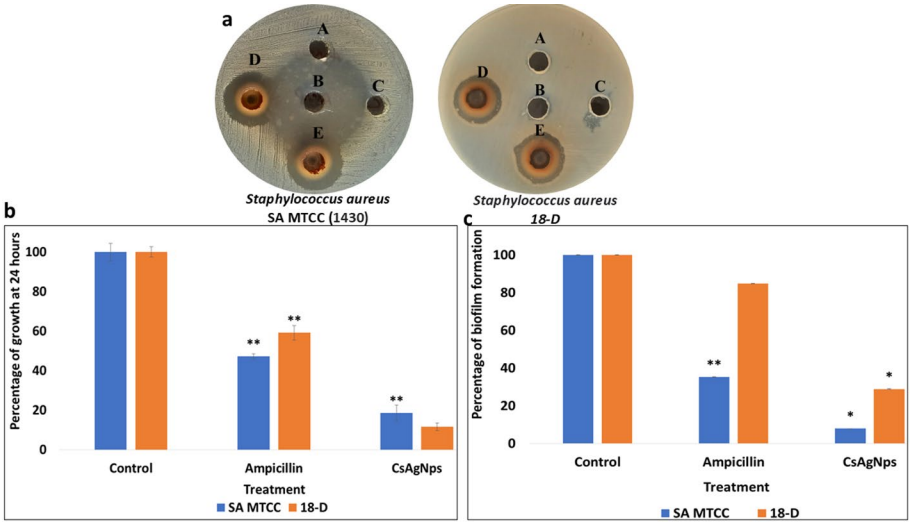

Fig. 7 Antibacterial and antibiofilm potential of CsAgNps: **a** Screening the antibacterial activity of CsAgNps in *S. aureus* strains (18-D and SA MTCC) A- 50 µL of silver nitrate solution; B- 25 µL of Ampicillin (1 mg/mL); C- 50 µL DMSO as blank; D- 50 µL of CsAgNps (1 mg/mL) (Zone A); E- 75 µL of CsAgNps (1 mg/mL) (zone B). **b** Growth rate computed after 24 h of CsAgNps treatment in SA MTCC and 18-D. **c** Percentage of biofilm formation to analyze the antibiofilm activity of CsAgNps in *S. aureus* strains. Error bars represent means ± standard deviation. ** t test ($P < 0.01$)

HR-TEM images confirmed the morphology of the nanoparticles as spherical with the size around 26 nm (Fig. 6c). The SAED image showed the crystal lattice structure of the synthesized CsAgNps and the analysis revealed that the d spacing between two particles were 8.67 1/nm and 6.18 1/nm. (Fig. 6d) Biological activity of CsAgNps is influenced by a variety of parameters, including surface chemistry, size, shape, agglomeration, particle morphology, particle composition, cell type, etc., and these physicochemical qualities improve bioavailability, cellular absorption, and penetration, distribution, and overall therapeutic effects [30].

3.4 Antibacterial effect of CsAgNPs

The antibacterial ability of the synthesized CsAgNps was confirmed by using the agar well diffusion technique. *S. aureus* strains were examined (18-D and SA MTCC (1430)) and the antibacterial property of CsAgNps at various concentrations (50 µg/mL and 75 µg/mL) was confirmed by observing clear zones of inhibition. SA MTCC showed a zone of inhibition of 32 mm for ampicillin (control). Controls, including $AgNO_3$ and DMSO, showed no zones of inhibition (Fig. 7a). Ampicillin served as a positive control, representing a standard antibiotic to compare the antibacterial activity of the nanoparticles. Silver nitrate ($AgNO_3$) was used as a chemical control, since the nanoparticles were synthesized using $AgNO_3$. This helps determine whether any observed antibacterial activity is due to the nanoparticles themselves or simply the presence of silver ions. Dimethyl sulfoxide (DMSO) was used as a solvent control, as the nanoparticles were later dissolved in 10% DMSO. This ensures that any antibacterial effect is not due to the solvent alone. The zone of inhibition for SA MTCC (1430) showed the diameter of clearance of 20 mm and 24 mm and for 18-D, it was 18 mm and 19 mm at the concentrations of 50 µg/mL and 75 µg/mL respectively. Generally, AgNPs provoke concerns about the potential adverse impact on human health. But when they are produced by green synthesis, they have less harmful effects. CsAgNps have comparatively lower cytotoxicity than other antibiotics in normal

cells. This may be because of the natural compounds in the *Camellia sinensis* extract that are present in the CsAgNps [31]. Due to their small size in the nanometer range, larger surface area, and other unique physicochemical properties, these silver nanoparticles exhibited antibacterial properties, which led to the disruption of bacterial cells because of the formation of gaps on the membrane. The capacity of the synthesized nanoparticles to adhere to the bacterial cell membrane was correlated with bacterial protein degradation and cell permeability [32].

The MIC readings were acquired visually based on the turbidity present in the 96 well plates and were found as 0.78 µg/mL for 18-D and 1.56 µg/mL for SA MTCC. The growth rates were computed by plotting the graph for 24 h through the absorbance reading obtained at 600 nm in a multi-mode reader. (Fig. 7b). The CsAgNps-treated wells were compared to control and ampicillin treatment. Tested strains showed an 81% and 88% decrease in growth percentage compared to the control in SA MTCC and 18-D respectively. The strains in the CsAgNps-treated wells grew at a far slower rate than the others. The MBC shows the lowest bactericidal concentration of *S. aureus* bacteria required to totally kill the bacterial cells. MBC values were found as 12.5 µg/mL for both 18-D and SA MTCC strains. MIC and MBC confirmed the antibacterial activity of the CsAgNps and its capacity to inhibit and kill *S. aureus* bacterial strains.

Gram-positive microorganisms have an overall negative charge because they contain teichoic acids. Strong interactions between CsAgNps phytocompounds and negatively charged cell wall components may explain the potent bactericidal effect of CsAgNps. Variable effects of AgNps on Gram-positive and Gram-negative bacteria may be attributable to differences in membrane structure and cell wall composition, which may affect AgNP availability [33]. The ability of CsAgNps to permeate the bacterial membrane resulted in structural injury to the membrane. This also led to the leakage of cellular contents, such as cell organelles, resulting in cell lysis [34].

The percentage of biofilm formation was reduced by 71% for 18-D and 92% for SA MTCC. These results revealed that the nanoparticles exhibited effective antibacterial effects in all the tested strains, including antibiotic-resistant strains 18 D. The rate of biofilm development was also dramatically decreased for all tested strains. Thus, the bacteriostatic, bactericidal and antibiofilm formation properties of CsAgNps in *S. aureus* strains were clearly demonstrated in in vitro studies. Due to the reduced size of the synthesized silver nanoparticles, they have a greater surface area and consequently greater contact with the cellular membrane, resulting in greater damage. AgNps interferes with the thiol (-SH) groups of proteins and enzymes in the bacterial cell wall and enters the cytoplasm, CsAgNps interacts with proteins, DNA, and other biomolecules within the cell. Due to the ability of CsAgNps to deactivate enzymes, numerous signaling and metabolic pathways which are responsible for biofilm formation. The degradation of chromosomal DNA by synthesized AgNps renders the bacteria incapable of reproduction. AgNps can also generate reactive oxygen species, resulting in cellular oxidative stress. Additionally, it impacts the bacterial cell's respiratory processes [33]. CsAgNps exhibited potent bacteriostatic and bactericidal properties in MIC and MBC assays. CsAgNps inhibits biofilm formation, as demonstrated by the confirmation of its anti-biofilm activity (Fig. 7c). This study has proved that synthesized CsAgNps effectively controlled the growth and biofilm in the challenging Gram-positive *S. aureus.*

The efficacy of CsAgNps in disrupting the biofilms depends on major factors including size, shape, charge and phytocompounds of *C. sinensis* extract. The first and foremost drawback of antibiotics is penetration into the biofilm matrix. This can easily be overcome by nanosized particles. The synthesized CsAgNps was spherical with a negative charge that can easily breach into extracellular polymeric substance (EPS) layer. The physical interaction of CsAgNps with EPS layer disrupts the polysaccharide and protein layers of EPS. The negative charged particles interact with positive charged components of EPS layer and destabilize the whole network [35]. In future, CsAgNps coated medical implants can be developed to prevent the formation of biofilms from the initial phase by interfering with the bacteria's ability to adhere to surfaces, the nanoparticles can stop the early phases of biofilm formation which is very helpful in avoiding infections in medical implants and devices.

4 Conclusion

Green synthesis is one of the growing needs for an environmentally friendly and sustainable form of nanotechnology-based approach to find alternatives to antibiotics. Conventional chemical techniques frequently use hazardous chemicals and energy, which are harmful to the environment and human health. Plant extract mediated nanoparticles provide a safer and more environmentally friendly alternative that supports to reduce environmental impact. In addition to lowering waste and toxicity, green synthesis strategy promotes the development of eco-friendly nanomaterials for wide range of biomedical applications. The growth of antimicrobial-resistant strains has promoted a search for new antibiotics that are cost-effective, biocompatible, and effective against antibiotic-resistant bacteria. By harnessing the synergistic potential of CsAgNps, we envision a promising avenue for combating Gram-positive antibiotic-resistant bacterial pathogens and advancing the frontiers of medical science. Phytocompounds of *Camellia sinensis* extract were identified by using LC MS analysis. In silico studies, insights into the interaction between *Camellia sinensis* phytocompounds and bacterial proteins affirm the antibacterial potential of these compounds. In vitro studies on synthesis of CsAgNps confirmed the potent antibacterial and antibiofilm effect on tested *S. aureus* strains even at lower concentration. The anti-bacterial efficacy of CsAgNps as determined by this research in treating these bacteria is of utmost importance in the treatment of Gram positive bacterial infections. CsAgNps-incorporated products can be developed and commercialized as CsAgNps-incorporated gels, CsAgNps-incorporated creams, etc. to control infections caused by antibiotic-resistant Gram positive pathogens. Hence, CsAgNps may be further explored in in-vivo conditions to develop an effective, ecofriendly alternative nanomedicine to treat a variety of bacterial infections. The limitations of the research work can be addressed by exploring the scalability and reproducibility of the green synthesis method by using *Camellia sinensis* leaf extract mediated nanoparticle synthesis. Future directions include investigating the mechanism for enhanced antimicrobial activity in multidrug pathogens, assessing the biocompatibility in vivo studies, and exploring the potential applications for slow and sustained release of the drugs.

Acknowledgements
Authors are thankful to B.S. Abdur Rahman Institute of Science & Technology, Chennai for providing research facilities in School of life sciences.

Author contributions
"SH conceived and designed research. TJ, and SR conducted experiments. SH analyzed data. All authors wrote the manuscript. All authors read and approved the manuscript."

Data availability
Data will be available on request from the corresponding author.

Declarations

Consent for publication
All authors read and approved the manuscript for publication.

Competing interests
The authors declare that there is no competing interests.

Received: 26 January 2025 / Accepted: 30 May 2025
Published online: 12 June 2025

References

1. Malik S, Muhammad K, Waheed Y. Nanotechnology: a revolution in modern industry. Molecules. 2023;28(2):661. https://doi.org/10.3390/molecules28020661.
2. Abbas R, Luo J, Qi X, Naz A, Khan IA, Liu H, Yu S, Wei J. Silver nanoparticles: synthesis, structure, properties and applications. Nanomaterials. 2024;14(17):1425. https://doi.org/10.3390/nano14171425.
3. Fahim M, Shahzaib A, Nishat N, Jahan A, Bhat TA, Inam A. (2024). Green synthesis of silver nanoparticles: a comprehensive review of methods, influencing factors, and applications. JCIS Open, 100125.
4. Osman AI, Zhang Y, Farghali M, et al. Synthesis of green nanoparticles for energy, biomedical, environmental, agricultural, and food applications: a review. Environ Chem Lett. 2024;22:841–87. https://doi.org/10.1007/s10311-023-01682-3.
5. Attallah NGM, Elekhnawy E, Negm WA, Hussein IA, Mokhtar FA, Al-Fakhrany OM. In vivo and in vitro antimicrobial activity of biogenic silver nanoparticles against *Staphylococcus aureus* clinical isolates. Pharmaceuticals. 2022;15(2):194. https://doi.org/10.3390/ph15020194. PMID: 35215306; PMCID: PMC8878289.
6. Hairil Anuar AH, Abd Ghafar SA, Hanafiah RM, Lim V, Mohd Pazli NFA. Critical evaluation of green synthesized silver Nanoparticles–Kaempferol for antibacterial activity against Methicillin-Resistant *Staphylococcus aureus*. Int J Nanomed. 2024;19:1339–50. PMID: 38348172; PMCID: PMC10860521.
7. Lade H, Kim JS. Bacterial targets of antibiotics in Methicillin–Resistant *Staphylococcus aureus*. Antibiot. 2021;10(4):398. https://doi.org/10.3390/antibiotics10040398.
8. Ahmed SK, Hussein S, Qurbani K, Ibrahim RH, Fareeq A, Mahmood KA, Mohamed MG. Antimicrobial resistance: impacts, challenges, and future prospects. J Med Surg Public Health. 2024;2:100081.
9. Dzobo K. The role of natural products as sources of therapeutic agents for innovative drug discovery. Compr Pharmacol. 2022;408–22. https://doi.org/10.1016/B978-0-12-820472-6.00041-4.
10. Chaudhary P, Mitra D, Mohapatra PKD, Docea AO, Myo EM, Janmeda P, Cho WC. Camellia sinensis: insights on its molecular mechanisms of action towards nutraceutical, anticancer potential and other therapeutic applications. Arab J Chem. 2023;16(5):104680.
11. Kong C, Zhang H, Li L, Liu Z. Effects of green tea extract epigallocatechin-3-gallate (EGCG) on oral disease-associated microbes: a review. J Oral Microbiol. 2022;14(1):2131117. https://doi.org/10.1080/20002297.2022.2131117.
12. Rodrigues AS, Batista JGS, Rodrigues MÁV, Thipe VC, Minarini LAR, Lopes PS, Lugão AB. Advances in silver nanoparticles: a comprehensive review on their potential as antimicrobial agents and their mechanisms of action elucidated by proteomics. Front Microbiol. 2024;15:1440065. https://doi.org/10.3389/fmicb.2024.1440065.
13. Juzer T, Ranjani S, Hemalatha S. Camellia sinensis mediated synthesis and characterization of nanoparticles and applications to control Gram-negative ESBL producing antibiotic resistant bacterial pathogens. Food Bioscience. 2022;50:102070.
14. Soundharajan R, Srinivasan H. Camellia sinensis mediated nanoparticles to control growth and biofilm in Vibrio Sp. Aquacult Int. 2025;33(3):1–19.
15. Harborne AJ. Phytochemical methods a guide to modern techniques of plant analysis. Springer science & business media; 1998.
16. Santhanalakshmi RS, Hemalatha S. Anti-bacterial activity of *Cymbopogon citratus* nanoparticles against Vibrio species infecting aquatic organisms. Aquat Toxicol. 2023;260:106583. https://doi.org/10.1016/j.aquatox.2023.106583.
17. Sri vidhyaa KS, Ranjani S, Hemalatha S. *Citrus limon* phytocompounds decorated nanoparticles control poultry pathogens arch. Microbiol. 2023;205:123. https://doi.org/10.1007/s00203-023-03462-7.
18. Harine A, Ranjani S, Hemalatha S. Antifungal efficacy of citrusfusion mediated silver nanoparticles in Candida species. BMC Biotechnol. 2025;25(1):18.
19. Soundhararajan R, Srinivasan H. Multidrug-resistant Bacillus species isolated from hospital soil environment is controlled by nanobiotics incorporated nanoformulation. Environ Res. 2024;246:118122.
20. Basha SBA, Soundhararajan R, Srinivasan H. Solanum virginianum mediated green nanoparticles to control dental pathogens. Discover Appl Sci. 2025;7(1):67.
21. Kathija N, Ranjani S, Hemalatha S. Endophytic Fungi lasiodiplodia theobromae–Mediated efagnps as potent antibacterial agent against MDR Klebsiella pneumoniae. BioNanoScience. 2024;14(1):276–86.
22. Kumar D, Soundhararajan R, Srinivasan H. Screening the efficacy of platinum-based nanomaterial synthesized from *Allium sativum* to control plant pathogens. J Mater Science: Mater Eng. 2024;19(1):29.
23. Alaabedin AAZ, Majeed AMA, Hamza BH. Green synthesis of silver nanoparticles and their effect on the skin determined using IR thermography. Kuwait J Sci. 2024;51(1):100076.

24. Alex AM, Subburaman S, Chauhan S, Ahuja V, Abdi G, Tarighat MA. Green synthesis of silver nanoparticle prepared with Ocimum species and assessment of anticancer potential. Sci Rep. 2024;14(1):11707.
25. Patterson AL. The scherrer formula for X-ray particle size determination. Phys Rev. 1939;56(10):978.
26. XRD Crystallite. (grain) Size calculator (Scherrer equation)—InstaNANO. https://instanano.com/all/characterization/xrd/crystallite-size/ (accessed May 2nd, 2025).
27. Lv C, Wang K, Zhao X, Wang F. Damage-accumulation-induced crack propagation and fatigue life analysis of a porous LY12 aluminum alloy plate. Materials. 2024;17(1):192. https://doi.org/10.3390/ma17010192.
28. Savvidou MG, Kontari E, Kalantzi S, Mamma D. Green synthesis of silver nanoparticles using the cell-free supernatant of *Haematococcus pluvialis* culture. Materials. 2024;17(1):187. https://doi.org/10.3390/ma17010187.
29. Raja S, Ramesh V, Thivaharan V. Green biosynthesis of silver nanoparticles using Calliandra haematocephala leaf extract, their antibacterial activity and hydrogen peroxide sensing capability. Arab J Chem. 2017;10(2):253–61.
30. Menichetti A, Mavridi-Printezi A, Mordini D, Montalti M. Effect of size, shape and surface functionalization on the antibacterial activity of silver nanoparticles. J Funct Biomaterials. 2023;14(5):244. https://doi.org/10.3390/jfb14050244.
31. Abdelwahab MA, Nabil A, El-Hosainy H, Tahway R, Taha MS. Green synthesis of silver nanoparticles using curcumin: a comparative study of antimicrobial and antibiofilm effects on *Acinetobacter baumannii* against chemical conventional methods. Results Chem. 2024;7:101274.
32. Dhaka A, Mali SC, Sharma S, Trivedi R. A review on biological synthesis of silver nanoparticles and their potential applications. Results Chem. 2023;6:101108.
33. More PR, Pandit S, Filippis A, Franci G, Mijakovic I, Galdiero M. Silver nanoparticles: bactericidal and mechanistic approach against drug resistant pathogens. Microorganisms. 2023;11(2):369. https://doi.org/10.3390/microorganisms11020369.
34. Mikhailova EO. Green silver nanoparticles: an antibacterial mechanism. Antibiotics. 2025;14(1):5. https://doi.org/10.3390/antibiotics14010005.
35. Hosnedlova B, Kabanov D, Kepinska M, Narayanan B, Parikesit VH, Fernandez AA, Bjørklund C, Nguyen G, Farid HV, Sochor A, Pholosi J, Baron A, Jakubek M, M., Kizek R. (2022). Effect of Biosynthesized Silver Nanoparticles on Bacterial Biofilm Changes in *S. aureus* and *E. coli*. Nanomaterials , *12*(13), 2183. https://doi.org/10.3390/nano12132183

Publisher's note